Expression, purification, crystallization and preliminary X-ray diffraction analysis of carbonyl reductase from *Candida parapsilosis* ATCC 7330

Nidhi Aggarwal,[a] P. K. Mandal,[b] Namasivayam Gautham[b] and Anju Chadha[a,c]*

[a]Department of Biotechnology, Indian Institute of Technology Madras, Chennai 600 036, India, [b]CAS in Crystallography and Biophysics, University of Madras, Guindy, Chennai 600 025, India, and [c]National Center for Catalysis Research, Indian Institute of Technology Madras, Chennai 600 036, India

Correspondence e-mail: anjuc@iitm.ac.in

The NAD(P)H-dependent carbonyl reductase from *Candida parapsilosis* ATCC 7330 catalyses the asymmetric reduction of ethyl 4-phenyl-2-oxobutanoate to ethyl (*R*)-4-phenyl-2-hydroxybutanoate, a precursor of angiotensin-converting enzyme inhibitors such as Cilazapril and Benazepril. The carbonyl reductase was expressed in *Escherichia coli* and purified by GST-affinity and size-exclusion chromatography. Crystals were obtained by the hanging-drop vapour-diffusion method and diffracted to 1.86 Å resolution. The asymmetric unit contained two molecules of carbonyl reductase, with a solvent content of 48%. The structure was solved by molecular replacement using cinnamyl alcohol dehydrogenase from *Saccharomyces cerevisiae* as a search model.

1. Introduction

Optically pure chiral alcohols are important intermediates for the synthesis of pharmaceuticals and agrochemicals (Nakamura *et al.*, 2003; Patel, 2006). Carbonyl reductases reduce carbonyl compounds to optically pure alcohols. Hence, they find their application in organic synthesis. The enantioselectivity of carbonyl reductases depends on the structural composition of the substrate binding site, which in turn determines the positioning of the large and small substituents of prochiral ketones. Depending on the face of hydride transfer, either *R* or *S* alcohols are formed by reduction of prochiral ketones. There are a limited number of reports on *R*-specific carbonyl reductases (Li *et al.*, 2010; Inoue *et al.*, 2005). On the other hand, the *S*-specific reductases are widely reported (Kaluzna *et al.*, 2004).

Ethyl (*R*)-4-phenyl-2-hydroxybutanoate is a precursor of angiotensin-converting enzyme (ACE) inhibitors such as Cilazapril and Benazepril. The advantages associated with biocatalytic methods (enantioselectivity, regioselectivity and chemoselectivity) make them a preferred choice for the synthesis of drug precursors in comparison to chemical methods. Recently, Li *et al.* (2010) and Richter & Hummel (2011) reported enantioselective reduction of ethyl 4-phenyl-2-oxobutanoate to ethyl (*R*)-4-phenyl-2-hydroxybutanoate using carbonyl reductase isolated from *Candida krusei* and *Neurospora crassa*.

We have demonstrated that *Candida parapsilosis* ATCC 7330 is a versatile biocatalyst that reduces aromatic and aliphatic keto-esters and aromatic ketones in moderate to excellent enantioselectivities, depending on substrate structure (Baskar *et al.*, 2004; Kaliaperumal *et al.*, 2011; Mahajabeen & Chadha, 2011; Saravanan *et al.*, 2010). A novel *R*-specific carbonyl reductase (*Cp* CR) was isolated from this yeast (Chadha *et al.*, unpublished results) which shares 40.0% sequence identity with cinnamyl alcohol dehydrogenase from *Saccharomyces cerevisiae* (PDB entry 1piw, Valencia *et al.*, 2004). Unlike the known cinnamyl alcohol dehydrogenases, *Cp* CR reduces α-keto-ester (ethyl 4-phenyl-2-oxobutanoate, EOPB) to the optically pure alcohol [ethyl (*R*)-4-phenyl-2-hydroxybutanoate] in 99.0% enantiomeric excess. *Cp* CR exists as a dimer like other cinnamyl alcohol dehydrogenases (Valencia *et al.*, 2004; Bomati & Noel, 2005). To explain the structural basis for the enantioselectivity of this enzyme, we have carried out crystallization and X-ray diffraction analysis of this carbonyl reductase.

Table 1
Diffraction data-collection and processing statistics.

Values in parentheses are for the highest-resolution shell.

Space group	$P2_12_12_1$
Resolution (Å)	25.00–1.86 (1.93–1.86)
Unit-cell parameters (Å)	$a = 65.72$, $b = 99.89$, $c = 116.66$
Total no. of reflections	308427
No. of unique reflections	62705
R_{merge}† (%)	8.9 (59.4)
Mean $I/\sigma(I)$	5.46 (2.13)
Completeness (%)	96.1 (97.7)
Multiplicity	4.9 (4.6)
No. of molecules in asymmetric unit	2
V_M (Å^3 Da^{-1})	2.37
Solvent content (%)	48.78

† $R_{merge} = \sum_{hkl} \sum_i |I_i(hkl) - \langle I(hkl)\rangle| / \sum_{hkl} \sum_i I_i(hkl)$.

2. Materials and methods

2.1. Protein expression and purification

The Cp CR gene (http://www.yeastgenome.org/cgi-bin/locus.fpl?locus=ADH6) was amplified using the genomic DNA of *C. parapsilosis* ATCC 7330 as a template. The Cp CR was amplified using the primers F-5′-**AGATCT**ATGACTAAAGCAGTACCAGACAAG-3′ (*Bgl*II) and 5′-TGTGAGTAGACAAGGTTTG**CTCGAG**-3′ (*Xho*I). The amplified product was cloned in the pGEMT vector followed by sub-cloning in pGEX-6-P-1. The BL21 cells containing Cp CR were grown in Luria Bertani media until the OD$_{600}$ reached 0.6–0.8 at 310 K; overexpression was induced using 0.3 m*M* IPTG (isopropyl β-D-1-thiogalactopyranoside) at 296 K for 16 h.

The cells were harvested by centrifugation at 10 000 rev min^{-1} for 5 min. Protein purification was performed using a fast protein liquid chromatography (FPLC) system (ÄKTA purifier, GE Biosciences). All the purification steps were carried out at 277 K using buffer *A* (20 m*M* Tris pH 7.5, 500 m*M* NaCl, 4 m*M* MgCl$_2$, 5% glycerol, 1 m*M* DTT). Cells from 1 l culture were resuspended in 25 ml of buffer *A* and disrupted by ultra-sonication. The homogenate was centrifuged at 12 000 rev min^{-1} for 45 min. The cleared lysate was loaded onto a GST column (equilibrated with buffer *A*) at 0.2 ml min^{-1}. The column was washed with buffer *A* for 10 column volumes. The recombinant protein was eluted with 50 m*M* Tris (pH 8.0) containing 25 m*M* glutathione. GST-carbonyl reductase was desalted with buffer *B* (20 m*M* Tris, 50 m*M* NaCl, 1 m*M* DTT pH 7.5) and digested with PreScission protease (GE Life Sciences) for 12–16 h at 277 K. The Cp CR after PreScission protease cleavage contains five non-native residues (GPLGS) originating from the pGEX-6-P-1 vector. The PreScission protease digested samples were loaded onto Superdex 200 equilibrated with 20 m*M* Tris, 50 m*M* NaCl, 1 m*M* DTT pH 7.5. The active fractions from gel filtration were loaded onto the GST column equilibrated with buffer *A*. The flow-through containing the 40 kDa protein was pooled, concentrated and desalted with buffer *B*. The carbonyl reductase concentrated (10 kDa molecular-weight cutoff; Amicon) to 13.5 mg ml^{-1} was used for crystallization experiments. The purified protein samples were analysed by SDS–PAGE followed by Coomassie Brilliant Blue R250 staining (Fig. 1). The protein concentration was calculated using the Bradford method (Bradford, 1976).

2.2. Crystallization and X-ray data collection

Crystallization trials of the purified protein were performed using the hanging-drop vapour-diffusion method at 293 K. Rectangular rod-shaped crystals (Fig. 2) were obtained when 1 µl of the protein sample (13.5 mg ml^{-1}) was mixed with an equal volume of reservoir solution and equilibrated against 1 ml of the latter. The reservoir solution consisted of 25%(*w*/*v*) PEG 4000 as a precipitant, 0.1 *M* HEPES pH 7.5 as buffer, and 8% isopropanol and 0.1 m*M* ZnCl$_2$ as additives.

The crystals were soaked in a cryoprotectant solution prepared by mixing 1 µl of the reservoir solution and 1 µl of 50% glycerol and flash-cooled in a gaseous nitrogen stream at 93 K. X-ray diffraction data were collected on an R-AXIS IV++ imaging-plate system using Cu $K\alpha$ radiation (λ = 1.5418 Å) generated by the rotating-anode Rigaku FR-E+ SuperBright X-ray generator at the X-ray Crystallography Facility in the Centre for Cellular and Molecular Biology, Hyderabad, India. The exposure time was 240 s per image and an oscillation range of 1° was used to collect 311 images at a crystal-to-detector distance of 130 mm. The diffraction data were processed using the program *HKL*-2000 (Otwinowski & Minor, 1997).
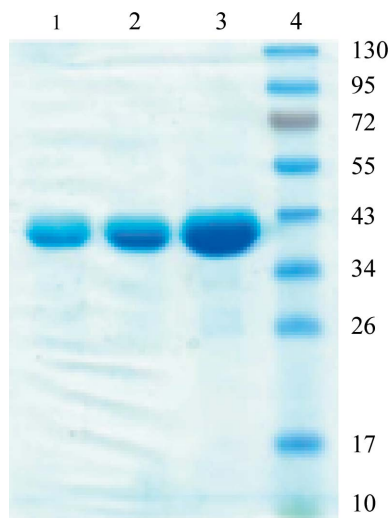

Figure 1
SDS–PAGE analysis of purified Cp CR. Lanes 1, 2, 3: 10, 17, 34 µg of purified Cp CR, respectively. Lane 4: molecular-weight marker (pre-stained marker from Fermentas) (given in kDa).
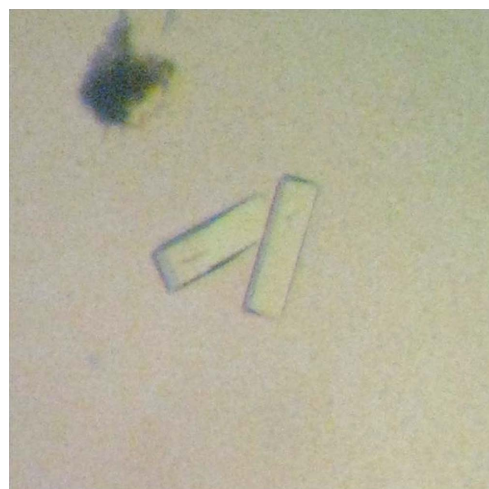

Figure 2
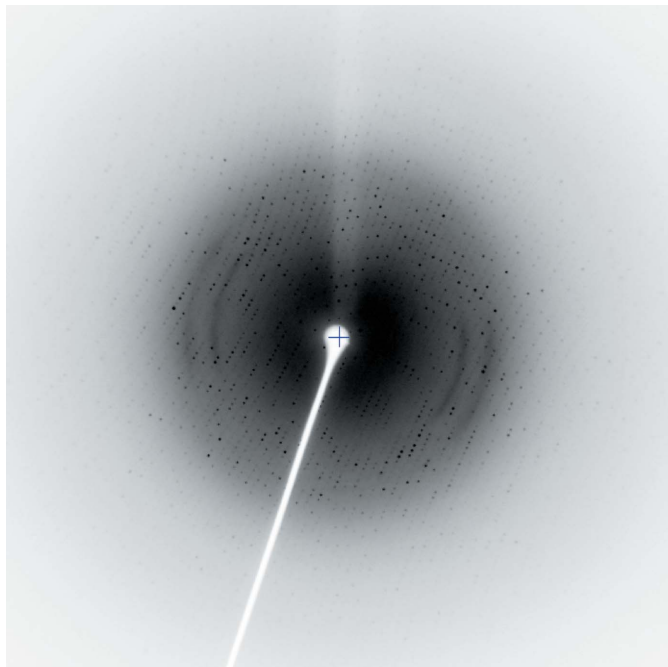Crystals of the Cp CR. The dimensions of the largest crystals are 0.04 × 0.06 × 0.22 mm.

Figure 3
Diffraction pattern of the *Cp* CR crystal taken at the X-ray Crystallography Facility, Centre for Cellular and Molecular Biology, Hyderabad, India.

Diffraction data-collection and processing statistics are given in Table 1.

3. Results and discussion

The crystals of *Cp* CR diffracted to a resolution of 1.86 Å (Fig. 3). The crystals belonged to the orthorhombic space group $P2_12_12_1$, with unit-cell parameters $a = 65.72$, $b = 99.89$, $c = 116.66$ Å. Based on the unit-cell volume and molecular mass of one *Cp* CR monomer, the Matthews coefficient (Matthews, 1968) was calculated to be 4.80 $Å^3\,Da^{-1}$, which suggested the presence of a dimer, and not a monomer, in the asymmetric unit. The solvent content was then calculated to be 48.78%. (The solution of the structure as a dimer confirms these parameters.) The structure was solved by molecular replacement (MR) using the program *Phaser* (Storoni *et al.*, 2004) in the *CCP*4 suite (Winn *et al.*, 2011), using the structure of the dimer of cinnamyl alcohol dehydrogenase from *S. cerevisiae* (PDB entry 1piw, Valencia *et al.*, 2004) as a search model. This had the highest sequence identity (40%) with *Cp* CR. The translation function *Z*-scores (TFZ) for the best and second-best MR solutions were 8.6 and 7.8, respectively. However, the best solution had no packing clashes (PAK = 0), while the second-best solution had a PAK value of 2. Model building and structure refinement are currently being carried out for *Cp* CR. Attempts are being made to crystallize this reductase in the presence of substrate analogues and inhibitors to understand the complete mechanism of the enzyme and the enantioselectivity.

References

Baskar, B., Pandian, N. G., Priya, K. & Chadha, A. (2004). *Tetrahedron Asymmetry*, **15**, 2961–2966.
Bomati, E. K. & Noel, J. P. (2005). *Plant Cell*, **17**, 1598–1611.
Bradford, M. M. (1976). *Anal. Biochem.* **72**, 248–254.
Inoue, K., Makino, Y. & Itoh, N. (2005). *Tetrahedron Asymmetry*, **16**, 2539–2549.
Kaliaperumal, T., Gummadi, S. N. & Chadha, A. (2011). *Tetrahedron Asymmetry*, **22**, 1548–1552.
Kaluzna, I. A., Matsuda, T., Sewell, A. K. & Stewart, J. D. (2004). *J. Am. Chem. Soc.* **126**, 12827–12832.
Li, N., Ni, Y. & Sun, Z. (2010). *J. Mol. Catal. B Enzym.* **66**, 190–197.
Mahajabeen, P. & Chadha, A. (2011). *Tetrahedron Asymmetry*, **22**, 2156–2160.
Matthews, B. W. (1968). *J. Mol. Biol.* **33**, 491–497.
Nakamura, K., Yamanaka, R., Matsuda, T. & Harada, T. (2003). *Tetrahedron Asymmetry*, **14**, 2659–2681.
Otwinowski, Z. & Minor, W. (1997). *Methods Enzymol.* **276**, 307–326.
Patel, R. N. (2006). *Curr. Opin. Drug Discov. Devel.* **9**, 741–764.
Richter, N. & Hummel, W. (2011). *Enzyme Microb. Technol.* **48**, 472–479.
Saravanan, T. & Chadha, A. (2010). *Tetrahedron Asymmetry*, **21**, 457–460.
Storoni, L. C., McCoy, A. J. & Read, R. J. (2004). *Acta Cryst.* D**60**, 432–438.
Valencia, E., Larroy, C., Ochoa, W. F., Parés, X., Fita, I. & Biosca, J. A. (2004). *J. Mol. Biol.* **341**, 1049–1062.
Winn, M. D. *et al.* (2011). *Acta Cryst.* D**67**, 235–242.